

A route to high gain photodetectors through suppressed recombination in disordered films

Bronson Philippa, Ron White, and Almantas Pivrikas

Citation: [Applied Physics Letters](#) **109**, 153301 (2016); doi: 10.1063/1.4963705

View online: <http://dx.doi.org/10.1063/1.4963705>

View Table of Contents: <http://scitation.aip.org/content/aip/journal/apl/109/15?ver=pdfcov>

Published by the [AIP Publishing](#)

Articles you may be interested in

[Charge transport and recombination in P3HT:PbS solar cells](#)

J. Appl. Phys. **117**, 095503 (2015); 10.1063/1.4913952

[High response organic ultraviolet photodetector based on blend of 4, 4', 4''-tri-\(2-methylphenyl phenylamino\) triphenylamine and tris-\(8-hydroxyquinoline\) gallium](#)

Appl. Phys. Lett. **93**, 103309 (2008); 10.1063/1.2980025

[High gain, broadband In Ga As/In Ga As P quantum well infrared photodetector](#)

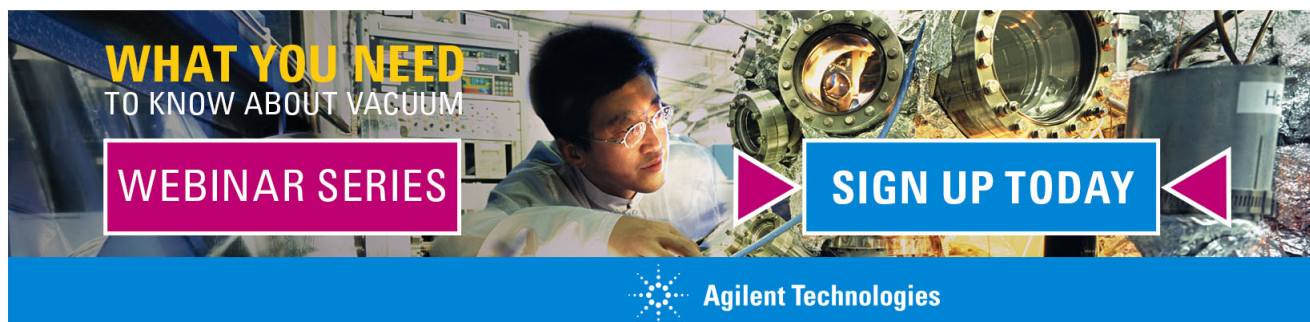
Appl. Phys. Lett. **89**, 081128 (2006); 10.1063/1.2338803

[Low-frequency noise gain and photocurrent gain in quantum well infrared photodetectors](#)

J. Appl. Phys. **86**, 6580 (1999); 10.1063/1.371624

[High gain-bandwidth-product silicon heterointerface photodetector](#)

Appl. Phys. Lett. **70**, 303 (1997); 10.1063/1.118399

A promotional banner for Agilent Technologies. It features a background image of a scientist in a lab coat working with a piece of equipment. Overlaid on the image are several text elements: 'WHAT YOU NEED TO KNOW ABOUT VACUUM' in yellow and white, 'WEBINAR SERIES' in white on a purple rectangular background, and 'SIGN UP TODAY' in white on a blue rectangular background. The Agilent Technologies logo and name are at the bottom.

A route to high gain photodetectors through suppressed recombination in disordered films

Bronson Philippa,¹ Ron White,² and Almantas Pivrikas^{3,a)}

¹College of Science, Technology and Engineering, James Cook University, Cairns 4870, Australia

²College of Science, Technology and Engineering, James Cook University, Townsville 4811, Australia

³School of Engineering and Information Technology, Murdoch University, Perth 6150, Australia

(Received 22 March 2016; accepted 14 September 2016; published online 10 October 2016)

Secondary photocurrents offer an alternative mechanism to photomultiplier tubes and avalanche diodes for making high gain photodetectors that are able to operate even at extremely low light conditions. While in the past secondary currents were studied mainly in ordered crystalline semiconductors, disordered systems offer some key advantages such as a potentially lower leakage current and typically longer photocarrier lifetimes due to trapping. In this work, we use numerical simulations to identify the critical device and material parameters required to achieve high photocurrent and gain in steady state. We find that imbalanced mobilities and suppressed, non-Langevin-type charge carrier recombination will produce the highest gain. A low light intensity, strong electric field, and a large single carrier space charge limited current are also beneficial for reaching high gains. These results would be useful for practical photodetector fabrication when aiming to maximize the gain. *Published by AIP Publishing.*
[\[http://dx.doi.org/10.1063/1.4963705\]](http://dx.doi.org/10.1063/1.4963705)

Solution processable semiconductors are attractive materials for photodetectors because of their potential for mechanical flexibility and the promise of low-cost, large area detectors.^{1,2} Recently, innovative photodetector designs have been demonstrated, such as the use of an insulating layer to produce a high-frequency detector that is insensitive to background illumination.^{3,4} Another advance has been the creation of narrowband detectors that use inefficient charge transport to engineer a sharp peak in external quantum efficiency (EQE) near the optical absorption edge of the active layer.^{5,6} However, these designs and others^{7,8} work by simply transporting the photogenerated charges through the device and have responsivities that are limited by the efficiencies of photon absorption, charge generation, and charge extraction. For photons with energies comparable to the bandgap, an absorbed photon can produce at most a single electron-hole pair.

In contrast, a photodetector utilising secondary photocurrents can achieve responsivities far exceeding one charge pair per photon.^{9,10} Photogeneration can trigger a large cascade of injected charges,^{11,12} resulting in EQEs much larger than one. To maximise the gain, the injected current must also be maximised, and hence we need Ohmic injection in a photodiode or a high conductivity photoconductor. Light-induced injection can also be achieved in reverse bias if photogenerated carriers fill traps in such a way as to lower the energy barrier for injection.^{13,14} Achieving high gain in reverse bias requires careful tuning of the energy levels, trap distribution, and interface properties. The high gain mode is comparatively simpler in forward bias and is likely to be applicable to a broader range of materials. Additionally, forward bias with Ohmic contacts will result in the maximum possible charge injection, improving the gain.

To date, the forward bias regime has rarely been considered in photodetectors made from novel solution processable materials. These materials have quite different properties to conventional semiconductors, such as much lower mobilities, different recombination nature (Langevin or suppressed Langevin), and generally rather imbalanced charge transport.^{15–17} The conditions to optimise the quantum efficiency of forward bias photodetectors in these materials are not well understood. This article aims to address that question and demonstrate the device parameters and operating conditions under which the gain is maximised.

We explore the design space of diode-geometry photodetectors using the well-known drift-diffusion model^{18–21} incorporating photogeneration, charge transport, recombination, and space charge effects. Our implementation has been described in previous publications^{22–24} so we will give only a brief summary here. We use a one-dimensional model and assume an effective homogenous medium for the active layer. Our objective is to model forward bias devices that achieve gain using the principle of charge neutralisation, so we apply a simplified geometry consisting of three layers: electrode/effective medium/electrode. The interfaces between the electrodes and the active layer are assumed to be Ohmic and are modelled with Boltzmann statistics.¹⁸ Ohmic contacts are necessary to maximise the gain because such contacts ensure the largest injection current.

Charge transport is described by drift and diffusion terms, where the diffusion coefficient is derived from the Einstein relation at room temperature. We neglect dispersive transport because the present simulations consider only steady-state behaviour. Recombination is bimolecular with the Langevin coefficient scaled by a reduction prefactor that will be varied during the simulations. In this work, photogeneration is taken to be uniform across the device, in other words, we simulate volume generation. We also tested Beer-Lambert absorption and found that the absorption profile has

^{a)}Author to whom correspondence should be addressed. Electronic mail: a.pivrikas@murdoch.edu.au

only a small impact upon the results. There is approximately a 10%–20% change in the gain across the range of $0 < \alpha d \leq 3$ (where α is the absorption coefficient and d is the active layer thickness). These changes are small compared to the influence of other parameters, so we consider only uniform generation ($\alpha d \rightarrow 0$). The recombination coefficient is assumed to be independent of film thickness, as would be the case for devices with uniform structural consistency. Light intensity is quantified by its concomitant charge generation, given in units of $CU_{\text{BI}}/t_{\text{tr}}^{\text{faster}}$ (where C is the device capacitance, U_{BI} is the built-in voltage, and $t_{\text{tr}}^{\text{faster}}$ is the transit time of faster carriers).

In this study, we have analysed low conductivity, undoped devices, in contrast with photoresistors that are typically highly doped and have Ohmic conduction. Consequently, in our devices, the dark conduction current is space charge limited ($j \propto V^2$) rather than Ohmic ($j \propto V$), the benefit being less injection current in the dark due to the low conductivity.

The operational principle of a high gain photodetector is shown by the current-voltage (IV) curves in Figure 1. The simulated device is a poor solar cell, having a low fill factor due to its imbalanced charge transport ($\mu_{\text{faster}}/\mu_{\text{slower}} = 100$, where μ indicates charge carrier mobility). Notably however, the forward bias photocurrent substantially exceeds the dark current. This device is a high-gain photodetector because the measurable current response is many times larger than the actual optical stimulation.

The high gain displayed in Figure 1 is the result of a secondary (injection) photocurrent. The physical mechanism of this gain is the following. In the dark, injection currents are space charge limited. In other words, the current is self-limiting: the injected charges screen the electric field and inhibit further injection. However, when light is applied to such a system, the photogenerated charges alter the electric field distribution and permit additional carriers to be injected. In this way, the injection current rises. Under the right circumstances (which are to be investigated below), the quantity of light-induced injected charges can greatly exceed the

quantity of photogenerated charges, and a high-gain device has been created.

In this work, we aim to optimise the gain of the photodetector to produce a large electrical response to a small optical stimulus. We define the gain as

$$\text{Gain} = \frac{j_{\text{light}} - j_{\text{dark}}}{Q_{\text{gen}}},$$

where j_{light} and j_{dark} are the currents under illumination and in the dark, respectively, and Q_{gen} is the photogeneration rate in units of charge per time.

To find out how to maximize the gain for various experimental parameters such as light intensity and mobility ratio, we now simulate photodetector gains across a range of conditions, as plotted in Figure 2. In reverse bias, the highest achievable gain is one, indicating that every photogenerated charge is being extracted. Gains less than one indicate recombination losses. Conversely, in forward bias, much higher gains can be achieved.

Figure 2(a) examines the impact of the light intensity, showing that the gain saturates at lower voltages when the light intensity is lower. Simply put, at lower voltages the gain is maximised when less light is applied. The light intensity is represented by the charge generation rate, i.e., the given value includes the quantum efficiencies of photon absorption and exciton separation. The charge generation rate is then normalised to $CU/t_{\text{tr}}^{\text{faster}}$, which is the approximate space charge limited injection current (SCLC) for a single charge carrier. Figure 2(a) shows that the photogeneration rate should be less than SCLC for high gain operation. This trend is explained by recombination: at lower light intensities, carrier lifetimes are longer, increasing the electrical gain that can be produced. We note that light intensities below SCLC are also necessary for high performance in *reverse bias* device operation.⁸

Figure 2(b) analyses the impact of electron and hole mobility ratio and shows that imbalanced charge transport is necessary for high gain operation. It is the electrostatic compensation of the slower carriers which permits injection of additional faster carriers; so if the mobility ratio $\mu_{\text{faster}}/\mu_{\text{slower}}$ is large, then many faster carriers will inject and transit during the lifetime of a single slower carrier. We emphasise that a low average mobility might arise due to trapping. These are steady-state simulations, so the mobility can be approximately considered as the average of the trapped and untrapped charges. If many charges are trapped, the average mobility will be low, contributing to high gain operation. Additionally, many disordered, solution-processable materials naturally have imbalanced mobilities. These characteristics are generally considered to be detrimental to performance, whereas here they are actually beneficial.

Recombination is the remaining charge transport parameter that has a crucial impact upon the gain. There are two recombination processes that must be considered: geminate (in which the recombining charge pairs originate from the same photon) and non-geminate (in which the recombining charges did not originate from the same photon). The process of geminate recombination is already incorporated into the net photogeneration rate, and therefore we now consider only the process of non-geminate recombination. This may

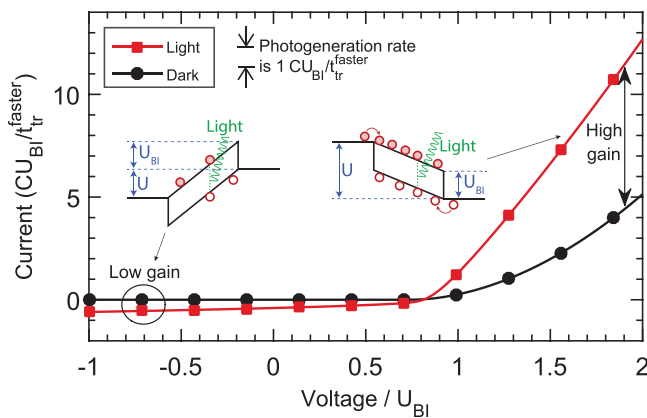


FIG. 1. The IV characteristic of a photodetector showing the regimes of low gain (in reverse bias) and high gain (in forward bias). In the case of reverse bias, the extraction current (circled) cannot exceed the photogeneration rate, which is indicated by the arrows near the legend. In contrast, in forward bias, the photocurrent is many times larger than the photogeneration rate, indicating that multiple charges are being extracted per absorbed photon. Simulation settings are a strongly imbalanced mobility ratio ($\mu_{\text{faster}}/\mu_{\text{slower}} = 100$) with non-Langevin recombination ($\beta_L/\beta = 100$). The inset shows simplified energy band diagrams for reverse bias (left hand side) and forward bias (right hand side), where U is the applied voltage.

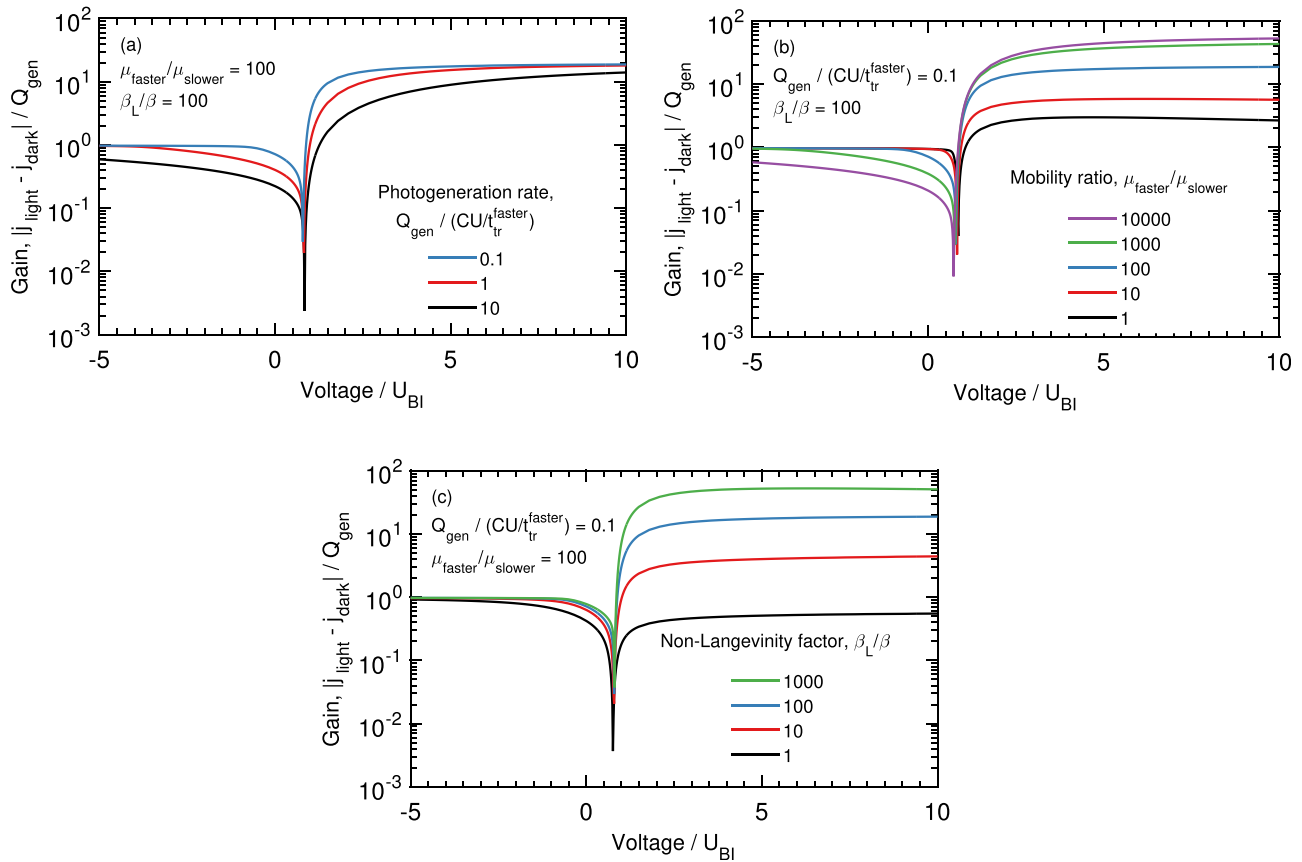


FIG. 2. The photogain can be maximized at (a) low light intensities and larger voltages and (b) imbalanced charge carrier mobilities. Both graphs show how the gain can exceed unity in forward bias, whereas in reverse bias, the gain merely measures the charge collection efficiency.

occur directly between charge carriers or may be mediated via trap states. In any case, there are two steps: first, the charges must meet, and second, they must recombine. If the former is the rate limiting step, then the recombination is described by the Langevin coefficient,²⁵ $\beta_L = e(\mu_{faster} + \mu_{slower})/\epsilon\epsilon_0$ where e is the charge of an electron and $\epsilon\epsilon_0$ is the permittivity. To model trap-assisted recombination, the mobility of the trapped carrier is set to zero.²⁶ We consider steady-state conditions in which there is an equilibrium of trapped and untrapped charges, so the mobilities μ_{faster} and μ_{slower} represent averages across the entire population of carriers. In this way, trap-assisted and direct band-to-band recombination may be considered simultaneously.

The second step in the recombination process is the interaction of the charges once they have approached within a distance smaller than the Coulomb radius.²⁷ If not every interaction results in recombination, then the recombination coefficient will deviate from the Langevin prediction.¹⁵ We define the non-Langevin factor β_L/β as the ratio of the Langevin coefficient β_L to the actual bimolecular recombination coefficient β . Higher values of β_L/β indicate more strongly suppressed recombination. Varying β_L/β in simulations allows for the impact of the recombination strength to be examined independently of other charge transport parameters.

Our results in Figure 3 show the impact of the recombination coefficient. It can be seen that a combination of

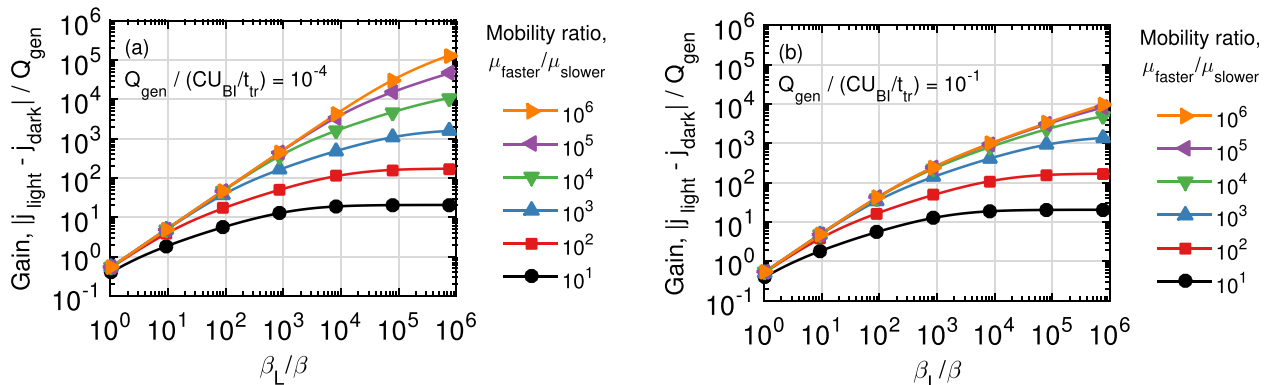


FIG. 3. Photocurrent gain dependence of photocarrier lifetime or recombination rate defined by recombination coefficient (β_L/β). The photodetector gain increases as the bimolecular recombination is suppressed. Plots (a) and (b) show different light intensities, as indicated on each plot. The correct combination of charge transport parameters will produce high photodetector gains. A constant voltage of $U/U_{BI} = 5$ was applied for these simulations.

strongly imbalanced charge transport and suppressed recombination is needed in order to maximise the gain.

Extremely high gains ($>10^5$) are possible, given appropriate charge transport parameters. The most demanding requirement is to achieve strongly suppressed recombination, i.e., large values of β_L/β . To put these values in context, reported β_L/β values include 10^2 to 10^3 in amorphous hydrogenated silicon,²⁸ 10^3 to 10^4 in polymer-fullerene systems,^{15,28} and 10^4 to 10^5 in organometal halide perovskites.^{29,30}

Furthermore, high gains can only be achieved if the charge generation rate remains low in comparison with SCLC (Figure 3(a)). If the charge generation rate becomes too large, then the gain is suppressed (Figure 3(b)). The reduction in gain occurs because space charge limits are reached despite the compensation of the photogenerated charges. The combination of high gain and high light intensity would require very large currents to flow. Such high currents cannot be sustained, and therefore the gain drops.

It is worth considering some implementation aspects that will affect the devices proposed here. There will be a continuous dark current in forward bias that needs to be subtracted from the measured current. This introduces additional complexity and measurement noise and will reduce the detectivity. However, this architecture does provide a mechanism to achieve extremely high gain photodetection. Notably, it is able to utilise materials with a strong mobility imbalance. Such an imbalance is generally considered detrimental for other applications such as solar cells.^{31,32} Therefore, there exist opportunities to use materials with attractive fabrication properties (such as solution processability) that may have been discarded as unsuitable for traditional photovoltaic or photodetection applications.

Another point to consider is the influence of traps. Traps may actually be beneficial for these devices if they act to decrease the slower carrier's average mobility. On the other hand, there is the concern of trap-assisted recombination. If that recombination follows the functional form of a Langevin-like expression with the trapped carrier's mobility set to zero,²⁶ then the overall photodetector gain is likely to follow a similar dependence as Figure 3.

In conclusion, we have presented design rules for high gain photodetectors operating in steady state that use secondary injection photocurrents as their operational mechanism. Imbalanced mobilities are not only beneficial but actually required for this application. The other crucial charge transport parameter is strongly suppressed recombination. In practice, this represents a challenge, because many disordered systems exhibit near-to-Langevin recombination. Recently strategies to overcome this limitation have been proposed,^{33–35} potentially allowing for strongly suppressed recombination even in disordered systems. Our results clearly show that the recombination coefficient fundamentally defines the photodetector gain, and efforts to produce high gain devices must consider the recombination coefficient as a crucial parameter.

Computational resources were provided by the James Cook University High Performance Computing Centre.

- ¹X. Gong, M. Tong, Y. Xia, W. Cai, J. S. Moon, Y. Cao, G. Yu, C.-L. Shieh, B. Nilsson, and A. J. Heeger, *Science* **325**, 1665 (2009).
- ²K. J. Baeg, M. Binda, D. Natali, M. Caironi, and Y. Y. Noh, *Adv. Mater.* **25**, 4267 (2013).
- ³L. Reissig, S. Dalgleish, and K. Awaga, *AIP Adv.* **6**, 015306 (2016).
- ⁴L. Hu, Y. Noda, H. Ito, H. Kishida, A. Nakamura, and K. Awaga, *Appl. Phys. Lett.* **96**, 243303 (2010).
- ⁵Q. Lin, A. Armin, P. L. Burn, and P. Meredith, *Nat. Photonics* **9**, 687 (2015).
- ⁶A. Armin, R. D. Jansen-van Vuuren, N. Kopidakis, P. L. Burn, and P. Meredith, *Nat. Commun.* **6**, 6343 (2015).
- ⁷D. H. Kim, K. S. Kim, H. S. Shim, C. K. Moon, Y. W. Jin, and J. J. Kim, *Appl. Phys. Lett.* **105**, 213301 (2014).
- ⁸M. Stolterfoht, A. Armin, B. Philippa, R. D. White, P. L. Burn, P. Meredith, G. Juška, and A. Pivrikas, *Sci. Rep.* **5**, 9949 (2015).
- ⁹P. Bhattacharya, *Semiconductor Optoelectronic Devices*, 2nd ed. (Prentice Hall, 1997).
- ¹⁰G. Rieke, *Detection of Light* (Cambridge University Press, Cambridge, 2002).
- ¹¹F. Guo, B. Yang, Y. Yuan, Z. Xiao, Q. Dong, Y. Bi, and J. Huang, *Nat. Nanotechnol.* **7**, 798 (2012).
- ¹²W. T. Hammond and J. Xue, *Appl. Phys. Lett.* **97**, 073302 (2010).
- ¹³L. Shen, Y. Zhang, Y. Bai, X. Zheng, Q. Wang, and J. Huang, *Nanoscale* **8**, 12990 (2016).
- ¹⁴L. Li, F. Zhang, J. Wang, Q. An, Q. Sun, W. Wang, J. Zhang, and F. Teng, *Sci. Rep.* **5**, 9181 (2015).
- ¹⁵A. Pivrikas, N. S. Sariciftci, G. Juška, and R. Österbacka, *Prog. Photovoltaics* **15**, 677 (2007).
- ¹⁶D. Hertel and H. Bässler, *ChemPhysChem* **9**, 666 (2008).
- ¹⁷P. W. M. Blom, V. D. Mihailetschi, L. J. A. Koster, and D. E. Markov, *Adv. Mater.* **19**, 1551 (2007).
- ¹⁸L. Koster, E. Smits, V. Mihailetschi, and P. Blom, *Phys. Rev. B* **72**, 085205 (2005).
- ¹⁹I. Hwang, C. R. McNeill, and N. C. Greenham, *J. Appl. Phys.* **106**, 094506 (2009).
- ²⁰M. T. Neukom, N. A. Reinke, and B. Ruhstaller, *Sol. Energy* **85**, 1250 (2011).
- ²¹M. T. Neukom, S. Züfle, and B. Ruhstaller, *Org. Electron.* **13**, 2910 (2012).
- ²²B. Philippa, M. Stolterfoht, P. L. Burn, G. Juška, P. Meredith, R. D. White, and A. Pivrikas, *Sci. Rep.* **4**, 5695 (2014).
- ²³B. Philippa, C. Vijila, R. D. White, P. Sonar, P. L. Burn, P. Meredith, and A. Pivrikas, *Org. Electron.* **16**, 205 (2015).
- ²⁴B. Philippa, M. Stolterfoht, R. D. White, M. Velusamy, P. L. Burn, P. Meredith, and A. Pivrikas, *J. Chem. Phys.* **141**, 054903 (2014).
- ²⁵G. Lakhwani, A. Rao, and R. H. Friend, *Annu. Rev. Phys. Chem.* **65**, 557 (2014).
- ²⁶M. Kuik, L. Koster, G. Wetzelaer, and P. Blom, *Phys. Rev. Lett.* **107**, 256805 (2011).
- ²⁷J. J. M. van der Holst, F. W. A. van Oost, R. Coehoorn, and P. A. Bobbert, *Phys. Rev. B* **80**, 235202 (2009).
- ²⁸G. Juška, K. Arlauskas, J. Stucklik, and R. Österbacka, *J. Non-Cryst. Solids* **352**, 1167 (2006).
- ²⁹A. Paulke, S. D. Stranks, J. Kniepert, J. Kurpiers, C. M. Wolff, N. Schön, H. J. Snaith, T. J. K. Brenner, and D. Neher, *Appl. Phys. Lett.* **108**, 113505 (2016).
- ³⁰C. Wehrenfennig, G. E. Eperon, M. B. Johnston, H. J. Snaith, and L. M. Herz, *Adv. Mater.* **26**, 1584 (2014).
- ³¹J. D. Kotlarski, D. J. D. Moet, and P. W. M. Blom, *J. Polym. Sci., Part B: Polym. Phys.* **49**, 708 (2011).
- ³²W. Tress, K. Leo, and M. Riede, *Phys. Rev. B* **85**, 155201 (2012).
- ³³T. M. Clarke, C. Lungenschmied, J. Peet, N. Drolet, and A. J. Mozer, *J. Phys. Chem. C* **119**, 7016 (2015).
- ³⁴M. Stolterfoht, B. Philippa, S. Shoaee, H. Jin, W. Jiang, R. D. White, P. L. Burn, P. Meredith, and A. Pivrikas, *J. Phys. Chem. C* **119**, 26866 (2015).
- ³⁵T. M. Burke, S. Sweetnam, K. Vandewal, and M. D. McGehee, *Adv. Energy Mater.* **5**, 1 (2015).